# AIMH Lab 2022 Activities for Healthcare

Fabio Carrara[1,*], Luca Ciampi[1], Marco Di Benedetto[1], Fabrizio Falchi[1], Claudio Gennaro[1] and Giuseppe Amato[1]

[1]ISTI-CNR, via G. Moruzzi, 1, Pisa, 56100, Italy

Abstract

The application of Artificial Intelligence technologies in healthcare can enhance and optimize medical diagnosis, treatment, and patient care. Medical imaging, which involves Computer Vision to interpret and understand visual data, is one area of healthcare that shows great promise for AI, and it can lead to faster and more accurate diagnoses, such as detecting early signs of cancer or identifying abnormalities in the brain. This short paper provides an introduction to some of the activities of the Artificial Intelligence for Media and Humanities Laboratory of the ISTI-CNR that integrate AI and medical image analysis in healthcare. Specifically, the paper presents approaches that utilize 3D medical images to detect the behavior-variant of frontotemporal dementia, a neurodegenerative syndrome that can be diagnosed by analyzing brain scans. Furthermore, it illustrates some Deep Learning-based techniques for localizing and counting biological structures in microscopy images, such as cells and perineuronal nets. Lastly, the paper presents a practical and cost-effective AI-based tool for multi-species pupillometry (mice and humans), which has been validated in various scenarios.

**Keywords**

AI for Healthcare, Medical Image Analysis, Computer Vision, Deep Learning

## 1. Introduction

Artificial Intelligence (AI) is rapidly transforming many industries, including healthcare. AI refers to using computer algorithms to simulate intelligent behavior. When applied to healthcare, these technologies can be used to enhance and optimize medical diagnosis, treatment, and patient care.

One area belonging to healthcare where AI is particularly promising is medical imaging, which involves Computer Vision (CV). CV specifically focuses on teaching computers to interpret and understand visual data from the world around us. Medical imaging plays a crucial role in diagnosing and treating many medical conditions. However, interpreting medical images can be a time-consuming and complex process, and even experienced experts can sometimes miss subtle changes that indicate disease. This is where Artificial Intelligence (AI) and Computer Vision come in. These technologies can be used to enhance and optimize medical imaging, enabling faster and more accurate diagnoses, such as detecting early signs of cancer or identifying structural abnormalities in the brain [1, 2, 3, 4]. In addition, AI and CV can help reduce the workload of radiologists and other medical professionals. By automating certain aspects of the image analysis process, such as identifying regions of interest or flagging potentially abnormal findings, these technologies can enable medical professionals to focus their time and attention on the most critical cases.

This short paper is a gentle introduction to some of the activities of the Artificial Intelligence for Media and Humanities Laboratory of the ISTI-CNR that connect AI and medical image analysis to healthcare. Specifically, we present some approaches dealing with 3D medical images to detect the *behavior-variant of frontotemporal dementia*, a neurodegenerative syndrome possible to diagnose by analyzing brain scans. Then, we illustrate some Deep Learning-based techniques aimed at localizing and counting cells from microscopy images, a step that can be useful to assist in cytotoxicity estimation. Furthermore, we describe an approach that can estimate the number of perineuronal nets, i.e., extracellular matrix aggregates surrounding the cell body of many neurons whose alteration is considered responsible for psychiatric disorders like schizophrenia. Finally, we show a cheap and practical AI-based tool to perform multi-species pupillometry (mice and humans), validating it in several scenarios.

## 2. 3D Image Analysis

In this line of research, we focus on complex representations of medical data, that is, volumetric structures, such as computed tomography (CT) or magnetic resonance (MR) 3D images, coming from acquiring patients' body parts.

Specifically, in [5], we focused on several neural network architectures to detect, from brain scans, the

*Ital-IA 2023: 3rd National Conference on Artificial Intelligence, organized by CINI, May 29–31, 2023, Pisa, Italy*

*Corresponding author.

fabio.carrara@isti.cnr.it (F. Carrara); giuseppe.amato@isti.cnr.it (G. Amato)

0000-0001-5014-5089 (F. Carrara); 0000-0002-6985-0439 (L. Ciampi); 0000-0001-5781-7060 (M. D. Benedetto); 0000-0001-6258-5313 (F. Falchi); 0000-0002-3715-149X (C. Gennaro); 0000-0003-0171-4315 (G. Amato)

*behavior-variant of the frontotemporal dementia* (bvFTD), a neurodegenerative syndrome whose clinical diagnosis remains a challenging task, especially in the early stage of the disease. Currently, the presence of frontal and anterior temporal lobe atrophies on magnetic resonance imaging (MRI) is part of the diagnostic criteria for bvFTD. However, MRI data processing is usually dependent on the acquisition device and mostly requires human-assisted crafting of feature extraction. Following the impressive improvements of deep architectures, in our study, we reported on bvFTD identification using various classes of artificial neural networks, and we presented the results achieved on classification accuracy and obliviousness on acquisition devices using extensive hyperparameter search. As shown in Figure 1, we demonstrated the stability and generalization of different deep networks based on the attention mechanism, where data intra-mixing confers models the ability to identify the disorder even on MRI data in inter-device settings, i.e., on data produced by different acquisition devices and without model fine-tuning.

In more recent times, we are also studying how brain anomaly detection techniques based on neural architectures, e.g., Generative Adversarial Networks (GANs) or Masked Auto Encoders (MAEs), can be used to enrich the diagnosis toolbox of medicians with nowadays standards and off-the-shelves equipment.

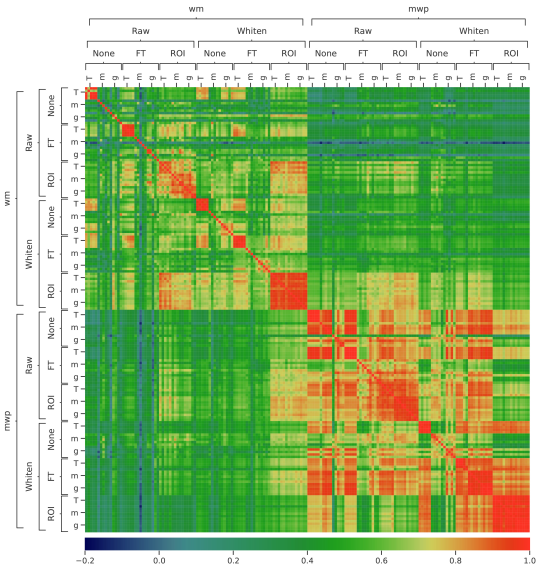


**Figure 1:** bvFTD: Pearson Correlation Coefficients among predictions of various transformer-based models. T = ViT, m = MLP-Mixer, g = gMLP. For each configuration, we report five runs with randomly initialized weights. Note that when ROI processing is used, predictions tend to correlate highly independently from the model or random weight initialization used. .

## 3. Counting Biological Structures in Microscopy Images

Detection and counting of biological structures in microscopy images is an analysis of considerable interest in biology and medicine. For instance, a viable cell count is a fundamental step in diagnosing several diseases, and it can be exploited to assist in cytotoxicity estimation, i.e., the quality of being toxic to cells. To this end, in [6], we investigated several counting approaches that have been successfully exploited in the literature over three public collections of microscopy images containing marked cells (see Figure 2 for some samples), assessing not only their counting performance compared to several state-of-the-art methods but also their ability to localize the counted cells correctly. Our analysis showed that counting errors do not always agree with the localization performance, and relying only on the counting metrics can lead to SOTA models producing incorrect cell localization. Therefore, we suggest measuring the mean average precision, or at least a grid average mean absolute error [7], to help practitioners develop better models and guide users to choose the model most tailored to their needs.

This dataset has been presented in [10] and comprises 100 RGB microscopy H&E stained histology images of

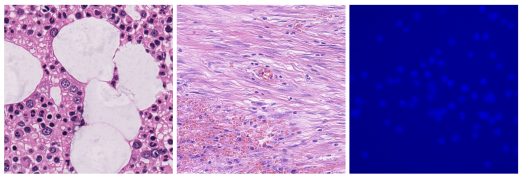

**Figure 2:** Some samples of the data used for counting cells in microscopy images. From left to right, (i) the *Modified Bone Marrow (MBM) Cells* [8, 9], a dataset of the human bone marrow tissues pertaining to 8 different patients; (ii) the *Nuclei Cells* dataset [10] comprising RGB microscopy H&E stained histology images of colorectal adenocarcinomas; (iii) the *VGG Cells* dataset [11], a synthetic collection of fluorescence microscopy images emulating bacterial cells.

colorectal adenocarcinomas having a common size of $500 \times 500 \times 3$. The images refer to 9 different patients. They have been cropped from non-overlapping areas representing a variety of tissue appearances from normal and malignant regions. Still, they also comprise areas with artifacts, over-staining, and failed autofocussing to simulate realistic outliers. Another peculiarity of this dataset is that the nuclei of the cells belong to four different categories, presenting different visual characteristics; some experts have manually annotated them by putting a dot over the centroids of each biological structure for a

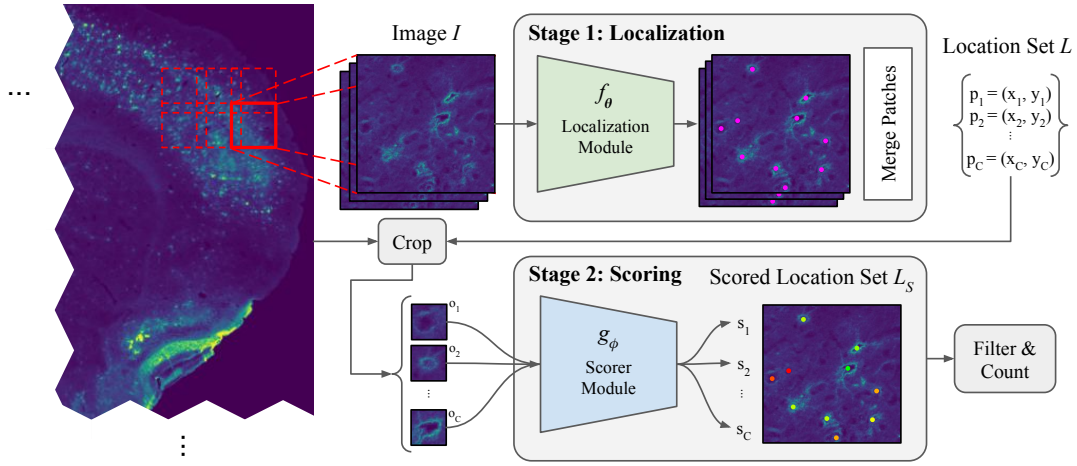


**Figure 3:** Proposed pipeline for detecting and counting PNNs in microscopy images under weakly-labeled data settings.

total of 29,756 nuclei marked. In the following, we refer to this dataset as *Nuclei Cells* dataset.

Furthermore, the AIMH Lab, in collaboration with the Institute of Neuroscience (IN-CNR), is researching Deep Learning-based approaches able to automatically evaluate the number of perineuronal nets (PNNs) in microscopy images. Specifically, PNNs are extracellular matrix aggregates surrounding the cell body of a large number of neurons [12, 13], and their alterations are associated with psychiatric disorders such as schizophrenia [14]. In [15], we proposed a two-stage counting methodology for counting PNNs in weakly-labeled data settings. We show the proposed pipeline in Figure 3. In the first stage, we adopted existing state-of-the-art solutions natively designed for detecting and counting cells trained over single-rater weakly-labeled data, i.e., containing annotation errors due to the difficulty in finding the correct patterns, even among experts. In the second stage, using a small set of multi-rater data, i.e., data labeled by multiple annotators, we defined a rescoring model aimed at refining predictions of the previous stage, increasing the correlation between the scores assigned by the model to the predictions and the raters' agreement on the sample labels. Finally, very recently, we presented a comprehensive atlas of PNN distribution and colocalization with parvalbumin (PV) cells for over 600 regions of adult mouse brains that offers a novel resource for understanding the organizational principles of the brain extracellular matrix [16].

## 4. Pupillometry

Pupillometry is an innovative non-invasive technique that measures changes in pupil size in response to various stimuli, providing insight into the functioning of the central nervous system. Pupil size is regulated by the sympathetic and parasympathetic nervous systems, which modulate the pupillary light reflex and the pupil response to cognitive and emotional stimuli. Pupillometry has been increasingly used in the assessment of various neuropsychiatric disorders, including autism spectrum disorder, attention deficit hyperactivity disorder, schizophrenia, and anxiety disorders.

In collaboration with the Institute of Neuroscience (IN-CNR), we developed cheap, practical, AI-based setups to perform multi-species pupillometry (mice and humans) and validated it in several scenarios [17].

In [18], we studied Cyclin-dependent kinase-like 5 (Cdkl5) deficiency disorder (CDD) — a severe neurodevelopmental disorder that causes early-onset seizures, intellectual disability, motor, and social impairment. No effective treatment is currently available, and medical management is only supportive. Recently, mouse models of CDD have been developed, demonstrating that mice lacking Cdkl5 exhibit autism-like phenotypes, hyperactivity, and dysregulation of the arousal system, providing the possibility to use these features as translational biomarkers. In this study, pupillometry was used to assess the integrity of the arousal system in CDD mice, and the results revealed a global defect in arousal modulation (see Figures 4 and 5). Therefore, pupillometry may provide an easy and valuable biomarker for the diagnosis and monitoring of CDD.

## 5. Conclusions

In this short paper, we reported some activities of the Artificial Intelligence for Media and Humanities (AIMH)

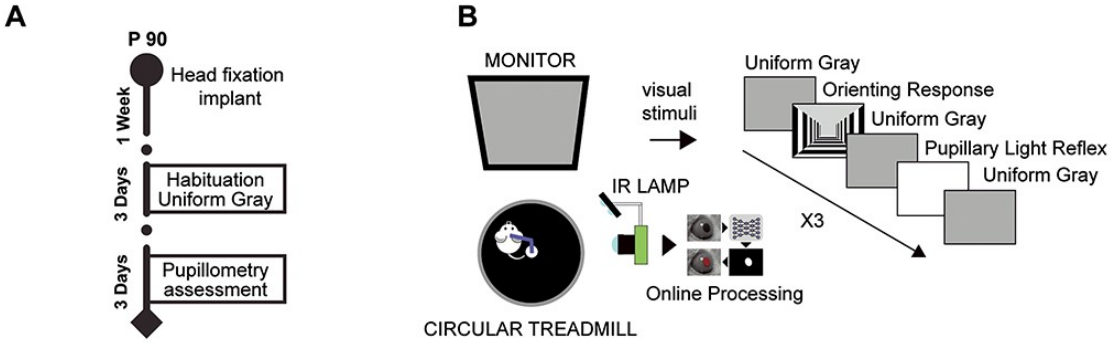


**Figure 4:** Locomotor activity and pupil size reveal arousal alterations in Cdkl5 male and female mutant mice. (A) Diagram showing the pupillometry timeline. (B) Schematic representation of the head-fixed pupillometry setup. The mouse was head-fixed to a custom-made metal arm equipped with a 3D-printed circular treadmill to monitor running behavior. In the meantime, we assessed: baseline pupil size (uniform gray screen), orienting response (to isoluminant virtual reality), and the pupillary light reflex (high luminance white screen). Each condition is repeated three times. We repeated the same protocol on three different days.

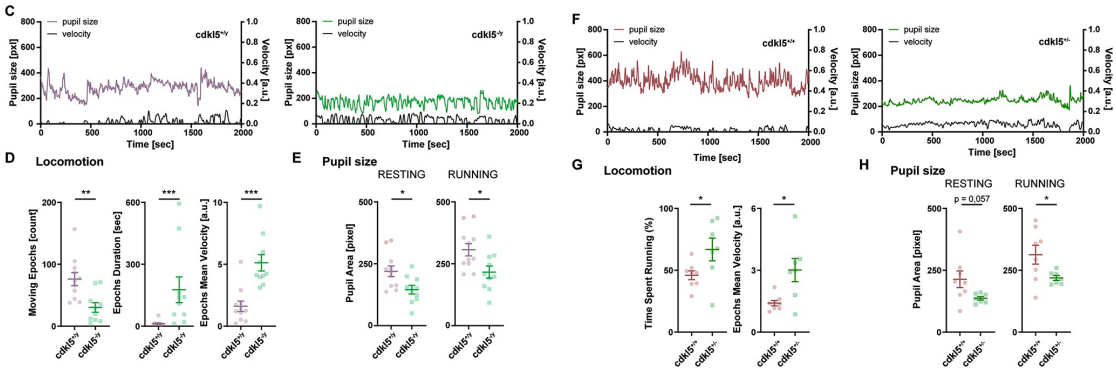


**Figure 5:** Locomotor activity and pupil size reveal arousal alterations in Cdkl5 male and female mutant mice. (C) Pupil diameter trace from a WT male mouse (Cdkl5−/y) and a Cdkl5 null male mouse (Cdkl5+/y). (D) Cdkl5 null mice showed alterations in locomotor activity compared to WT: a decreased number of moving epochs (defined as a period of continuous movement): P-value < 0.01, unpaired T-test; an increase in the average duration of moving epoch: P-value < 0.05, unpaired T-test; and an increase in epochs mean velocity: P-value < 0.001, unpaired T-test. (E) Cdkl5−/y showed a constitutively smaller pupil size compared to Cdkl5+/y both during resting and running (resting, P-value < 0.05; running, P-value < 0.05; unpaired T-test). (F) Pupil diameter trace from a WT female mouse (Cdkl5+/+) and a Cdkl5 heterozygous female mouse (Cdkl5+/−). (G) Cdkl5+/− mice showed an enhanced locomotor activity compared to Cdkl5+/+, in terms of percentage of time spent running, P-value < 0.05, unpaired T-test and velocity, P-value < 0.05, unpaired T-test. (H) Cdkl5+/− mice showed a baseline smaller pupil size compared to Cdkl5+/+ during running, P-value < 0.05, unpaired T-test, and a strong trend in resting, P-value = 0.057, unpaired T-test. n = 11 Cdkl5+/y, n = 10 Cdkl5−/y; n = 8 Cdkl5+/+, n = 7 Cdkl5+/−. *P-value < 0.05, **P-value < 0.01 and ***P-value < 0.001.

laboratory of the ISTI-CNR concerning Computer Vision approaches relying on Artificial Intelligence for medical image analysis. The proposed technologies can be used to enhance and optimize medical diagnosis, treatment, and patient care and represent valid tools exploitable by medical professionals. We described some approaches tackling the detection of the *behavior-variant of frontotemporal dementia* in 3D brain scans, some Deep Learning networks for counting biological structures, such as cells and PNNs, in microscopy images, and, finally, a cheap and practical AI-based tool to perform multi-species pupillometry (mice and humans).

## Acknowledgments

This work was partially supported by: PNRR - M4C2 - Investimento 1.3, Partenariato Esteso PE00000013 -

"FAIR - Future Artificial Intelligence Research" - Spoke 1 "Human-centered AI", funded by the European Union under the NextGenerationEU programme.

## References


[1] I. Maglogiannis, C. Doukas, Overview of advanced computer vision systems for skin lesions characterization, IEEE Transactions on Information Technology in Biomedicine 13 (2009) 721–733. URL: https://doi.org/10.1109%2Ftitb.2009.2017529. doi:10.1109/titb.2009.2017529.

[2] F. M. Calisto, C. Santiago, N. Nunes, J. C. Nascimento, Introduction of human-centric AI assistant to aid radiologists for multimodal breast image classification, International Journal of Human-Computer Studies 150 (2021) 102607. URL: https://doi.org/10.1016%2Fj.ijhcs.2021.102607. doi:10.1016/j.ijhcs.2021.102607.

[3] S. Jain, V. jagtap, N. Pise, Computer aided melanoma skin cancer detection using image processing, Procedia Computer Science 48 (2015) 735–740. URL: https://doi.org/10.1016%2Fj.procs.2015.04.209. doi:10.1016/j.procs.2015.04.209.

[4] P. K. Sethy, C. Pandey, M. R. Khan, S. K. Behera, K. Vijaykumar, S. Panigrahi, A cost-effective computer-vision based breast cancer diagnosis, Journal of Intelligent & Fuzzy Systems 41 (2021) 5253–5263. URL: https://doi.org/10.3233%2Fjifs-189848. doi:10.3233/jifs-189848.

[5] M. Di Benedetto, F. Carrara, B. Tafuri, S. Nigro, R. De Blasi, F. Falchi, C. Gennaro, G. Gigli, G. Logroscino, G. Amato, Deep networks for behavioral variant frontotemporal dementia identification from multiple acquisition sources, Computers in Biology and Medicine 148 (2022) 105937. URL: https://www.sciencedirect.com/science/article/pii/S0010482522006722. doi:https://doi.org/10.1016/j.compbiomed.2022.105937.

[6] L. Ciampi, F. Carrara, G. Amato, C. Gennaro, Counting or localizing? evaluating cell counting and detection in microscopy images, in: Proceedings of the 17th International Joint Conference on Computer Vision, Imaging and Computer Graphics Theory and Applications, SCITEPRESS - Science and Technology Publications, 2022. URL: https://doi.org/10.5220%2F0010923000003124. doi:10.5220/0010923000003124.

[7] R. Guerrero-Gómez-Olmedo, B. Torre-Jiménez, R. López-Sastre, S. Maldonado-Bascón, D. Oñoro-Rubio, Extremely overlapping vehicle counting, in: Pattern Recognition and Image Analysis, Springer International Publishing, 2015, pp. 423–431. URL: https://doi.org/10.1007%2F978-3-319-19390-8_48. doi:10.1007/978-3-319-19390-8_48.

[8] P. Kainz, M. Urschler, S. Schulter, P. Wohlhart, V. Lepetit, You should use regression to detect cells, in: Lecture Notes in Computer Science, Springer International Publishing, 2015, pp. 276–283. URL: https://doi.org/10.1007%2F978-3-319-24574-4_33. doi:10.1007/978-3-319-24574-4_33.

[9] J. P. Cohen, G. Boucher, C. A. Glastonbury, H. Z. Lo, Y. Bengio, Count-ception: Counting by fully convolutional redundant counting, in: 2017 IEEE International Conference on Computer Vision Workshops (ICCVW), IEEE, 2017. URL: https://doi.org/10.1109%2Ficcvw.2017.9. doi:10.1109/iccvw.2017.9.

[10] K. Sirinukunwattana, S. E. A. Raza, Y.-W. Tsang, D. R. J. Snead, I. A. Cree, N. M. Rajpoot, Locality sensitive deep learning for detection and classification of nuclei in routine colon cancer histology images, IEEE Transactions on Medical Imaging 35 (2016) 1196–1206. URL: https://doi.org/10.1109%2Ftmi.2016.2525803. doi:10.1109/tmi.2016.2525803.

[11] V. S. Lempitsky, A. Zisserman, Learning to count objects in images, in: Advances in Neural Information Processing Systems 23: 24th Annual Conference on Neural Information Processing Systems 2010. Proceedings of a meeting held 6-9 December 2010, Vancouver, British Columbia, Canada, Curran Associates, Inc., 2010, pp. 1324–1332. URL: https://proceedings.neurips.cc/paper/2010/hash/fe73f687e5bc5280214e0486b273a5f9-Abstract.html.

[12] C. M. Galtrey, J. C. F. Kwok, D. Carulli, K. E. Rhodes, J. W. Fawcett, Distribution and synthesis of extracellular matrix proteoglycans, hyaluronan, link proteins and tenascin-r in the rat spinal cord, European Journal of Neuroscience 27 (2008) 1373–1390. URL: https://doi.org/10.1111%2Fj.1460-9568.2008.06108.x. doi:10.1111/j.1460-9568.2008.06108.x.

[13] G. Köppe, G. Brückner, K. Brauer, W. Härtig, V. Bigl, Developmental patterns of proteoglycan-containing extracellular matrix in perineuronal nets and neuropil of the postnatal rat brain, Cell and Tissue Research 288 (1997) 33–41. URL: https://doi.org/10.1007%2Fs004410050790. doi:10.1007/s004410050790.

[14] S. Berretta, H. Pantazopoulos, M. Markota, C. Brown, E. T. Batzianouli, Losing the sugar coating: Potential impact of perineuronal net abnormalities on interneurons in schizophrenia, Schizophr. Res. 167 (2015) 18–27. doi:10.1016/j.schres.2014.12.040.

[15] L. Ciampi, F. Carrara, V. Totaro, R. Mazziotti, L. Lupori, C. Santiago, G. Amato, T. Pizzorusso, C. Gennaro, Learning to count biological struc-

tures with raters' uncertainty, Medical Image Analysis 80 (2022) 102500. URL: https://doi.org/10.1016%2Fj.media.2022.102500. doi:10.1016/j.media.2022.102500.

[16] L. Lupori, V. Totaro, S. Cornuti, L. Ciampi, F. Carrara, E. Grilli, A. Viglione, F. Tozzi, E. Putignano, R. Mazziotti, et al., A comprehensive atlas of perineuronal net distribution and colocalization with parvalbumin in the adult mouse brain, bioRxiv (2023) 2023–01.

[17] R. Mazziotti, F. Carrara, A. Viglione, L. Lupori, L. L. Verde, A. Benedetto, G. Ricci, G. Sagona, G. Amato, T. Pizzorusso, Meye: web app for translational and real-time pupillometry, eneuro 8 (2021).

[18] A. Viglione, G. Sagona, F. Carrara, G. Amato, V. Totaro, L. Lupori, E. Putignano, T. Pizzorusso, R. Mazziotti, Behavioral impulsivity is associated with pupillary alterations and hyperactivity in cdkl5 mutant mice, Human Molecular Genetics 31 (2022) 4107–4120.